Iterative Interstream Interference Cancellation for MIMO HSPA+ System

Hyougyoul Yu, Byonghyo Shim, Tae Won Oh
School of Information and Communication, Korea University
Anam-dong, Sungbuk-gu, Seoul, Korea, 136-713
Email: {hy_lyu, bshim, taewon}@korea.ac.kr

***Abstract*—In this paper, we propose an iterative interstream interference cancellation technique for system with frequency selective multiple input multiple output (MIMO) channel. Our method is inspired by the fact that the cancellation of the interstream interference can be regarded as a reduction in the magnitude of the interfering channel. We show that, as iteration goes on, the channel experienced by the equalizer gets close to the single input multiple output (SIMO) channel and, therefore, the proposed SIMO-like equalizer achieves improved equalization performance in terms of normalized mean square error. From simulations on downlink communications of 2×2 MIMO systems in HSPA UMTS standard, we show that the proposed method provides substantial performance gain over the conventional receiver algorithms.**

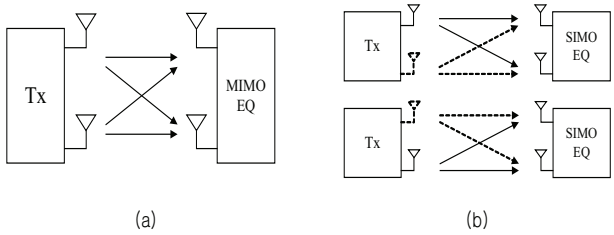

Fig. 1. The illustration of (a) conventional MIMO equalizer and (b) proposed method.

I. Introduction

Recently, increasing demand for high quality data services is fueling the deployment of high speed packet access (HSPA) standard in UMTS mobile communication systems. In the recent standard of HSPA referred to as HSPA+ [1], 2×2 multiple-input-multiple-output (MIMO) system [2] has been introduced to improve the average user throughput and the peak data rates. For achieving the target data rate (42Mbps) in frequency selective fading channel, an effective MIMO receiver technique that can effectively deal with intersymbol interference (ISI) and interstream interference is crucial. Traditionally, linear minimum mean square error (LMMSE) equalizer and its variants have long been employed, and these are still popularly being used owing to the benefit on complexity and implementation simplicity. However, because of the correlation between channels each stream is experiencing (e.g., rank loss due to small antenna spacing and/or the presence of strong line of sight component), in many situations, MIMO equalizer cannot properly handle the interstream interference resulting in substantial performance loss. Hence, an improved receiver algorithm that handles both ISI and interstream interferences is of great importance to meet the user demand and quality of service (QoS) of the HSPA+ based UMTS system.

Previous studies include iterative interference cancelation techniques and equalization [3]–[7]. The main focus of this approach is per code channel cancellation/suppression, either in serial [3], [5] or parallel manner [6], to reduce inter-user interference and improve signal-to-interference-and-noise ratio (SINR). While the key ingredient of these approaches lie on the minimum mean square error (MMSE) based equalization such as the MMSE successive interference cancellation (SIC) [3], recent focus has moved on to *a posteriori probability* (APP) detection via iterative detection and decoding (IDD). In the IDD scheme, the fast search algorithm so-called *list sphere decoding* (LSD) [8] is employed to perform efficient detection of the APP. The LSD algorithm has several variants including K-best detector [9] and LISt-Sequential (LISS) detector [5] (see, e.g., [7], for detailed discussion). Although the IDD is a promising option for systems with a narrowband flat-fading channel model such as the MIMO-OFDM systems, they may not be a good choice for MIMO systems with frequency selective channel response since the dimension of the channel matrix (roughly in the order of 10) is in general much larger than that of the MIMO-OFDM system (mostly 2×2 and 4×4) and also the dimension is not fixed because of channel variations.

The aim of this paper is to improve the performance of the CDMA systems with frequency selective MIMO channels using a cost effective interstream interference cancellation. Unlike the MMSE-SIC or MIMO-LMMSE equalizer, the proposed method gradually converts MIMO channel into two independent single-input-multiple-output (SIMO) channels by performing per stream interference cancellation iteratively (see Fig. 1). Since the SIMO channel equalizer is more robust to the channel correlation and also provides better MSE than the MIMO channel equalizer, the proposed equalizer outperforms the standard MIMO equalizer in terms of mean square error (MSE). In fact, using the simulations on downlink communication of UMTS HSPA+ system employing 2×2 MIMO transmission, we show that the proposed method offers substantial performance gain over the conventional approach.

The remainder of this paper is organized as follows. In Section II, the system model of the UMTS HSPA+ system and

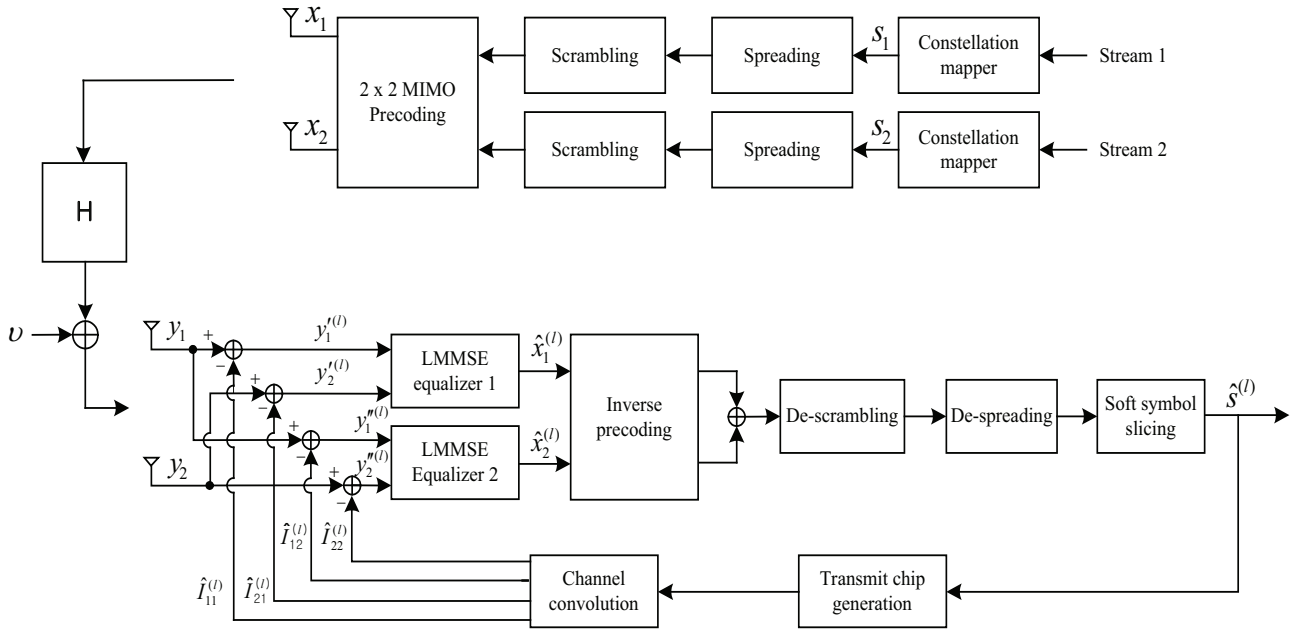

Fig. 2. The basic structure of the proposed scheme employing 2×2 MIMO in HSPA system.

the analysis of LMMSE equalizer in terms of the normalized mean square error are presented. In Section III, the proposed interstream interference cancelled SIMO equalization scheme is proposed. The simulation results and discussion are presented in Section IV and Section V concludes the paper.

We briefly summarize notations used in this paper. We employ uppercase and lowercase boldface letter for matrix and vector, respectively. Notations $(\cdot)^*$,$(\cdot)^H$,$(\cdot)^T$, and $(\cdot)^{-1}$ are used to denote the conjugate, Hermitian, transpose, and matrix inverse operations, respectively.

II. Downlink of UMTS HSPA System

A. System Model and LMMSE based MIMO Equalizer

In the HSPA+ system with the MIMO transmission mode, a precoding matrix is applied to two streams of Walsh coded and scrambled information vectors (see Fig. 2). By denoting the precoded transmit chip sequences as $x_1[n]$ and $x_2[n]$, respectively, the relationship between the transmit and received sequences at each receive antenna can be expressed as

$$\begin{aligned} y_1[n] &= \sum_k h_{11}[k]x_1[n-k] + \sum_k h_{12}[k]x_2[n-k] \\ &+ v_1[n] \qquad \text{(Antenna 1)} \quad (1) \\ y_2[n] &= \sum_k h_{21}[k]x_1[n-k] + \sum_k h_{22}[k]x_2[n-k] \\ &+ v_2[n] \qquad \text{(Antenna 2)} \quad (2) \end{aligned}$$

where $y_i[n]$ is the received signal for antenna i, $h_{ij}[n]$ is the overall channel impulse response (including transmit filter, propagation channel impulse response, and receiver filter) between the transmit antenna j and receive antenna i, and $v_i[n] \sim \mathcal{CN}(0, N_0)$ is the complex Gaussian noise vector.

For developing the LMMSE equalizer [10] of the MIMO-HSPA+ system, we use the following frequency domain representation as

$$\begin{aligned} y_1(\omega) &\approx h_{11}(\omega)x_1(\omega) + h_{12}(\omega)x_2(\omega) + v_1(\omega) \quad (3) \\ y_2(\omega) &\approx h_{21}(\omega)x_1(\omega) + h_{22}(\omega)x_2(\omega) + v_2(\omega) \quad (4) \end{aligned}$$

where $y_i(\omega)$, $x_i(\omega)$, $h_{ij}(\omega)$, and $v_i(\omega)$ are the discrete Fourier transform (DFT) of $y_i[n]$, $x_i[n]$, $h_{ij}[n]$, and $v_i[n]$, respectively. Note that an approximation error caused by the DFT of the linear convolution in (1) and (2) will be negligible if the DFT size chosen is much larger than the length of the overall channel impulse response [11]. Using the matrix-vector form, (3) and (4) can be simplified to

$$\mathbf{y}(\omega) = \mathbf{H}(\omega)\mathbf{x}(\omega) + \mathbf{v}(\omega) \quad (5)$$

where $\mathbf{y}(\omega) = [y_1^*(\omega)\ y_2^*(\omega)]^H$, and $\mathbf{H}(\omega) = [\mathbf{h}_1(\omega)\ \mathbf{h}_2(\omega)]$, where $\mathbf{h}_1(\omega) = [h_{11}^*(\omega)\ h_{21}^*(\omega)]^H$ and $\mathbf{h}_2(\omega) = [h_{12}^*(\omega)\ h_{22}^*(\omega)]^H$. Also, $\mathbf{x}(\omega) = [x_1^*(\omega)\ x_2^*(\omega)]^H$, and $\mathbf{v}(\omega) = [v_1^*(\omega)\ v_2^*(\omega)]^H$. In what follows, we drop ω and use $\mathbf{y} = \mathbf{H}\mathbf{x} + \mathbf{v}$ for notational simplicity.

The linear MMSE estimate $\hat{\mathbf{x}}$ of $\mathbf{x}$ is [12], [13]

$$\hat{\mathbf{x}} = R_{\mathbf{xy}}R_{\mathbf{yy}}^{-1}(\mathbf{y} - E[\mathbf{y}]). \quad (6)$$

Using $E[\mathbf{x}\mathbf{x}^H] = S\mathbf{I}$ and $E[|\mathbf{v}|^2] = N_0\mathbf{I}$, the crosscorrelation $R_{\mathbf{xy}}$ between $\mathbf{y}$ and $\mathbf{x}$ becomes $R_{\mathbf{xy}} = S\mathbf{H}^H$ and the autocorrelation of $\mathbf{y}$ is $R_{\mathbf{yy}} = \left(S\mathbf{H}\mathbf{H}^H + N_0\mathbf{I}\right)$. These together with the fact that $E[\mathbf{y}] = 0$, we have

$$\begin{aligned} \hat{\mathbf{x}} &= S\mathbf{H}^H\left(S\mathbf{H}\mathbf{H}^H + N_0\mathbf{I}\right)^{-1}\mathbf{y} \\ &= \frac{S}{N_0}\mathbf{H}^H\left(\frac{S}{N_0}\mathbf{H}\mathbf{H}^H + \mathbf{I}\right)^{-1}\mathbf{y}. \quad (7) \end{aligned}$$

By taking the inverse FFT of $\hat{\mathbf{x}}$, we can obtain the equalized chip sequence $\hat{x}[n]$.

B. NMSE Analysis of HSPA MIMO Equalizer

In this subsection, we investigate the asymptotic behavior of the LMMSE based MIMO equalizer for HSPA+ system for motivating our approach of interstream interference cancelled equalizer in Section III. Towards the end, we consider the normalized covariance $\mathcal{C}_{norm}(\mathbf{x},\hat{\mathbf{x}}) = \frac{1}{S}E[|\mathbf{x}-\hat{\mathbf{x}}|^2]$ of the LMMSE estimate in (7). It is well-known that $E[|\mathbf{x}-\hat{\mathbf{x}}|^2] = (\mathbf{R}_{\mathbf{xx}}^{-1} + \mathbf{H}^H\mathbf{R}_{\mathbf{vv}}^{-1}\mathbf{H})^{-1}$ [12] and hence

$$\begin{aligned}\mathcal{C}_{norm}(\mathbf{x},\hat{\mathbf{x}}) &= \frac{1}{S}\left(\frac{1}{S}\mathbf{I} + \frac{1}{N_0}\mathbf{H}^H\mathbf{H}\right)^{-1} \\ &= \left(\mathbf{I} + \mathrm{SNR}\mathbf{H}^H\mathbf{H}\right)^{-1} \end{aligned} \quad (8)$$

where $\mathbf{R}_{\mathbf{xx}} = S\mathbf{I}$, $\mathbf{R}_{\mathbf{vv}} = N_0\mathbf{I}$, and $\mathrm{SNR} = \frac{S}{N_0}$. Furthermore, if $\mathbf{h}_1$ and $\mathbf{h}_2$ denote the first and second column vectors of $\mathbf{H}$, respectively, then we have

$$\begin{aligned}\mathcal{C}_{norm}(\mathbf{x},\hat{\mathbf{x}}) &= (\mathbf{I} + \mathrm{SNR}\mathbf{H}^H\mathbf{H})^{-1} \\ &= \begin{bmatrix} 1+\mathrm{SNR}\|\mathbf{h}_1\|^2 & \mathrm{SNR}\mathbf{h}_1^H\mathbf{h}_2 \\ \mathrm{SNR}\mathbf{h}_2^H\mathbf{h}_1 & 1+\mathrm{SNR}\|\mathbf{h}_2\|^2 \end{bmatrix}^{-1}. \end{aligned} \quad (9)$$

Note that the $(1,1)$-th element of $\mathcal{C}_{norm}(\mathbf{x},\hat{\mathbf{x}})$, corresponding to the normalized mean square error (NMSE) of the first stream, is expressed as

$$\begin{aligned}&\mathrm{NMSE}(x_1,\hat{x}_1) \\ &= \frac{1+\mathrm{SNR}\|\mathbf{h}_2\|^2}{(1+\mathrm{SNR}\|\mathbf{h}_1\|^2)(1+\mathrm{SNR}\|\mathbf{h}_2\|^2) - \mathrm{SNR}^2|\mathbf{h}_1^H\mathbf{h}_2|^2} \\ &= \frac{1}{1+\mathrm{SNR}\|\mathbf{h}_1\|^2 - \frac{\mathrm{SNR}^2|\mathbf{h}_1^H\mathbf{h}_2|^2}{(1+\mathrm{SNR}\|\mathbf{h}_2\|^2)}} \\ &= \frac{1}{\mathrm{SNR}\left(\|\mathbf{h}_1\|^2 - \frac{|\mathbf{h}_1^H\mathbf{h}_2|^2}{\|\mathbf{h}_2\|^2+\frac{1}{\mathrm{SNR}}} + \frac{1}{\mathrm{SNR}}\right)}. \end{aligned} \quad (10)$$

Similarly, one can show that

$$\mathrm{NMSE}(x_2,\hat{x}_2) = \frac{1}{\mathrm{SNR}\left(\|\mathbf{h}_2\|^2 - \frac{|\mathbf{h}_2^H\mathbf{h}_1|^2}{\|\mathbf{h}_1\|^2+\frac{1}{\mathrm{SNR}}} + \frac{1}{\mathrm{SNR}}\right)}. \quad (11)$$

This result reveals that the equalizer performance depends not only on the SNR but also on the relationship between the two channel vectors $\mathbf{h}_1$ and $\mathbf{h}_2$. Let $\lambda(\mathbf{H},\mathrm{SNR}) = \left(\|\mathbf{h}_1\|^2 - \frac{|\mathbf{h}_1^H\mathbf{h}_2|^2}{\|\mathbf{h}_2\|^2+\frac{1}{\mathrm{SNR}}} + \frac{1}{\mathrm{SNR}}\right)$, then

$$\mathrm{NMSE}(x_1,\hat{x}_1) = \frac{1}{\mathrm{SNR}\lambda(\mathbf{H},\mathrm{SNR})}. \quad (12)$$

(12) provides direction for improvement. First, it is clear from (12) that two factors determining the performance of the LMMSE equalizer is the SNR and $\lambda(\mathbf{H},\mathrm{SNR})$, which is approximately a correlation between the two channel vectors.[1] While it is true that the correlation between the two channel vectors cannot be reduced directly, by canceling the second stream interference, we can effectively reduce the power of $\mathbf{h}_2$ (i.e., increase $\lambda(\mathbf{H},\mathrm{SNR})$) and hence achieves smaller NMSE.

[1]In the high SNR region, $\lambda(\mathbf{H},\mathrm{SNR})$ is approximated to $\|\mathbf{h}_1\|^2 - \frac{|\mathbf{h}_1^H\mathbf{h}_2|^2}{\|\mathbf{h}_2\|^2} = \|\mathbf{h}_1\|^2(1-\cos^2\theta)$ where θ is the angle between $\mathbf{h}_1$ and $\mathbf{h}_2$.

III. Iterative Interstream Interference Cancellation

The proposed scheme employs interstream interference cancellation to improve the equalizer performance. The key observation in our approach is that the cancellation of x_2 can be interpreted as the reduction in the magnitude of $\mathbf{h}_2$, which can be translated into reduction in the NMSE of x_1. In the same way, cancellation of x_1 will result in the reduction of the NMSE of x_2. To achieve this goal, two separate equalizers, one for x_1 estimation and the other for x_2 estimation, are employed (see Fig. 1). As shown in Fig. 2, the proposed scheme consists of two sets of equalizer followed by inverse precoding, channel despreader, symbol slicer, retransmission chain, and interference canceller.

A. Interstream Interference Cancellation

The cancellation process of the proposed method is done separately for each stream. In the input of the first equalizer for estimating x_1, the second stream is cancelled out and hence the new observation becomes

$$y_1' = h_{11}x_1 + h_{12}(x_2 - \hat{x}_2) + v_1 \quad (13)$$
$$y_2' = h_{21}x_1 + h_{22}(x_2 - \hat{x}_2) + v_2 \quad (14)$$

where $\hat{x}_2$ is the estimated stream of x_2. Similarly, the new observation for the second equalizer is

$$y_1'' = h_{11}(x_1 - \hat{x}_1) + h_{12}x_2 + v_1 \quad (15)$$
$$y_2'' = h_{21}(x_1 - \hat{x}_2) + h_{22}x_2 + v_2. \quad (16)$$

Since the treatment of y' and y'' is essentially same, we focus only on the y' in the sequel. Rewriting (7), the equalizer output $\hat{x}_2$ can be expressed as

$$\hat{x}_2 = \mathrm{SNR}\mathbf{h}_2^H\left(\mathrm{SNR}\mathbf{h}_1\mathbf{h}_1^H + \mathrm{SNR}\mathbf{h}_2\mathbf{h}_2^H + \mathbf{I}\right)^{-1}\mathbf{y}. \quad (17)$$

Using the matrix inversion lemma [14], (17) becomes,

$$\begin{aligned}\hat{x}_2 &= \frac{\mathrm{SNR}\mathbf{h}_2^H\Sigma^{-1}\mathbf{h}_2}{1+\mathrm{SNR}\mathbf{h}_2^H\Sigma^{-1}\mathbf{h}_2}x_2 + \frac{\mathrm{SNR}\mathbf{h}_2^H\Sigma^{-1}\mathbf{h}_1}{1+\mathrm{SNR}\mathbf{h}_2^H\Sigma^{-1}\mathbf{h}_2}x_1 \\ &+ \frac{\mathrm{SNR}\mathbf{h}_2^H\Sigma^{-1}}{1+\mathrm{SNR}\mathbf{h}_2^H\Sigma^{-1}\mathbf{h}_2}\mathbf{v} \end{aligned} \quad (18)$$

where $\Sigma = \mathrm{SNR}\mathbf{h}_1\mathbf{h}_1^H + \mathbf{I}$. Under the assumption that $\mathbf{h}_2^H\Sigma^{-1}\mathbf{h}_2$ is larger than $\mathbf{h}_2^H\Sigma^{-1}\mathbf{h}_1$ and $\mathbf{h}_2^H\Sigma^{-1}\mathbf{v}$, $\hat{x}_2 \approx \frac{\mathrm{SNR}\mathbf{h}_2^H\Sigma^{-1}\mathbf{h}_2}{1+\mathrm{SNR}\mathbf{h}_2^H\Sigma^{-1}\mathbf{h}_2}x_2$ and hence (13) and (14) becomes

$$y_1' \approx h_{11}x_1 + \beta h_{12}x_2 + v_1 \quad (19)$$
$$y_2' \approx h_{21}x_1 + \beta h_{22}x_2 + v_2 \quad (20)$$

where $\beta = \frac{1}{1+\mathrm{SNR}\mathbf{h}_2^H\Sigma^{-1}\mathbf{h}_2}$ indicates the amount of attenuation of the interstream interference x_2 in y'. The vector form of (19) and (20) is $\mathbf{y}' \approx \begin{bmatrix} \mathbf{h}_1 & \beta\mathbf{h}_2 \end{bmatrix}\mathbf{x} + \mathbf{v}$ and the NMSE in (10) is rewritten as

$$\mathrm{NMSE}(x_1,\hat{x}_1) = \frac{1}{\mathrm{SNR}\left(\|\mathbf{h}_1\|^2 - \frac{\beta^2|\mathbf{h}_1^H\mathbf{h}_2|^2}{\beta^2\|\mathbf{h}_2\|^2+\frac{1}{\mathrm{SNR}}} + \frac{1}{\mathrm{SNR}}\right)}. \quad (21)$$

As shown in Fig. 3(a), when β decreases, the denominator increases and thereby reduces $\mathrm{NMSE}(x_1,\hat{x}_1)$. General form

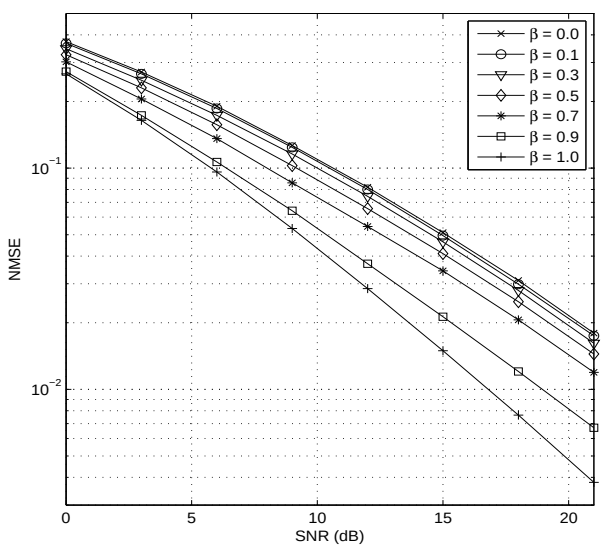

(a) NMSE as a function of β.

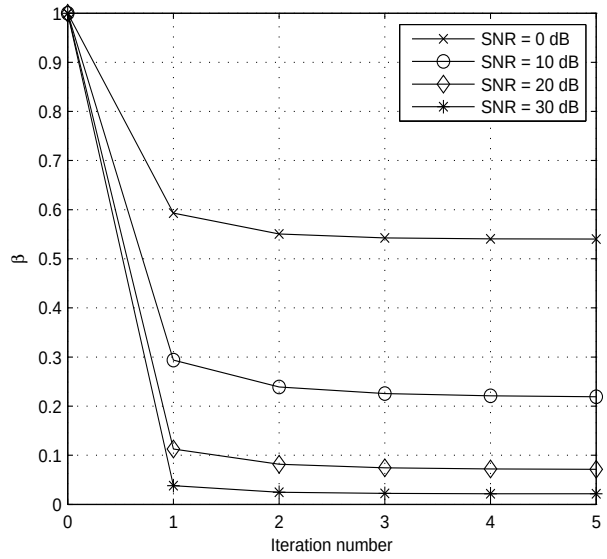

(b) β as a function of iteration number.

Fig. 3. NMSE and β as a function of SNR and iteration number, respectively

of the observation vector when we perform an iterative interstream cancellation is

$$\mathbf{y}^{(\ell+1)} \approx \left[\begin{array}{cc} \mathbf{h}_1 & \beta_\ell \mathbf{h}_2 \end{array} \right] \mathbf{x} + \mathbf{v} \tag{22}$$

where β_ℓ is the attenuation factor of the interstream interference x_2 at the ℓ-th iteration. Noting that $E[\left|x_2 - \hat{x}_2^\ell\right|^2] \approx E[|\beta_\ell\, x_2|^2] = \beta_\ell^2 S$ and also recalling that $\mathrm{NMSE}(x_2, \hat{x}_2) = \frac{1}{S} E[\left|x_2 - \hat{x}_2^\ell\right|^2]$, we have

$$\beta_{\ell+1} = \frac{1}{\sqrt{\mathrm{SNR}\left(\|\mathbf{h}_2\|^2 - \frac{\beta_\ell^2 |\mathbf{h}_2^H \mathbf{h}_1|^2}{\beta_\ell^2 \|\mathbf{h}_1\|^2 + \frac{1}{\mathrm{SNR}}} + \frac{1}{\mathrm{SNR}}\right)}}. \tag{23}$$

We observe from Fig. 3(b) that β decreases as the iteration number increases. However, it converges fast so that maximal performance gain can be achieved with only a few iterations.

B. Nonlinear MMSE based Soft Symbol Slicing and Retransmission

In order to ensure the performance improvement of the proposed method over the MIMO equalization technique, reliability of the symbol decision process should be guaranteed. Since it is well known that hard slicing often causes an error propagation [15], we employ the nonlinear MMSE estimation for symbol slicing. Denoting the input of symbol slicer as

$$\hat{r}_i[n] = s_i[n] + \upsilon_i[n] \tag{24}$$

where $s_i[n]$ and $\upsilon_i[n]$ are the symbol and noise after the equalization, inverse precoding, descrambling and despreading. The output of the NL-MMSE based soft slicer is [12]

$$\begin{aligned} \hat{s}_i[n] &= \arg\max_m E[s_m \,|\, \hat{r}_i] \\ &= \arg\max_m \frac{\Sigma_m s_m P(\hat{r}_i|s_m) P(s_m)}{\Sigma_m P(\hat{r}_i|s_m) P(s_m)}. \end{aligned} \tag{25}$$

Under the equal prior assumption on $P(s_m)$ and Gaussian model for $\upsilon_i[n]$, (25) becomes

$$\hat{s}_i[n] = \arg\max_m \frac{\Sigma_m s_m \exp\left(-\frac{|\hat{r}_i[n] - s_m|^2}{2\sigma_v^2}\right)}{\Sigma_m \exp\left(-\frac{|\hat{r}_i[n] - s_m|^2}{2\sigma_v^2}\right)} \tag{26}$$

where the noise power σ_v^2 can be obtained using the pilot signal as $\sigma_v^2 = \frac{1}{2} E[|\hat{r}_i[n] - \hat{r}_i[n-1]|^2]$. For a high SNR condition ($\frac{\sigma_{s_i}^2}{\sigma_v^2} \gg 1$), the MMSE estimate approximates to the hard decision since a single exponential term gets close to 1 while all other terms become negligible. On the contrary, as no dominant term exists for a code channel with low SNR, one can observe that $\hat{s}_i[n]$ is expressed as the sum of several terms and thus the magnitude of $\hat{s}_i[n]$ will be moderately small. Owing to the suppression of the unreliable symbol, the NL-MMSE symbol slicing is in general more robust to the error propagation than the hard decision based symbol slicing.

Finally, retransmission follows the footstep of the basestation transmission and is composed of Hadamard transform, scrambling, precoding, and convolution with the channel impulse response. The reconstructed interstream interferences used for x_1 and x_2 estimation are given by

$$\hat{I}_{i1}^{(\ell+1)}[n] = h_{i2}[n] * \hat{x}_2^{(\ell)}[n] \tag{27}$$

$$\hat{I}_{i2}^{(\ell+1)}[n] = h_{i1}[n] * \hat{x}_1^{(\ell)}[n] \tag{28}$$

where $\hat{x}_1^{(\ell)}$ and $\hat{x}_2^{(\ell)}$ are the retransmitted chip sequence at the ℓ-th iteration (see Fig. 2).

IV. Simulation Results and Discussion

A. Simulation Setup

In our simulation, we evaluate the performance of the proposed method in the downlink of the HSPA+ system. The

TABLE I
CHANNEL PARAMETERS FOR SIMULATIONS

ITU pedestrian A channel						
Tap	1	2	3	4	5	6
Relative delay (ns)	0	110	190	410	-	-
Average power (dB)	0.0	-9.7	-19.2	-22.8	-	-
ITU pedestrian B channel						
Tap	1	2	3	4	5	6
Relative delay (ns)	0	200	800	1200	2300	3700
Average power (dB)	0.0	-0.9	-4.9	-8.0	-7.8	-23.9

simulated propagation channel is generated based on the ITU Pedestrian A and B (Ped. A and B) model [16] (see table I). Seven physical layer data channels (HS-PDSCH) with QPSK modulation are used to generate a transmit datastream. As a measure for the performance, the bit error rate (BER) of data channels is used.

B. Simulations Results

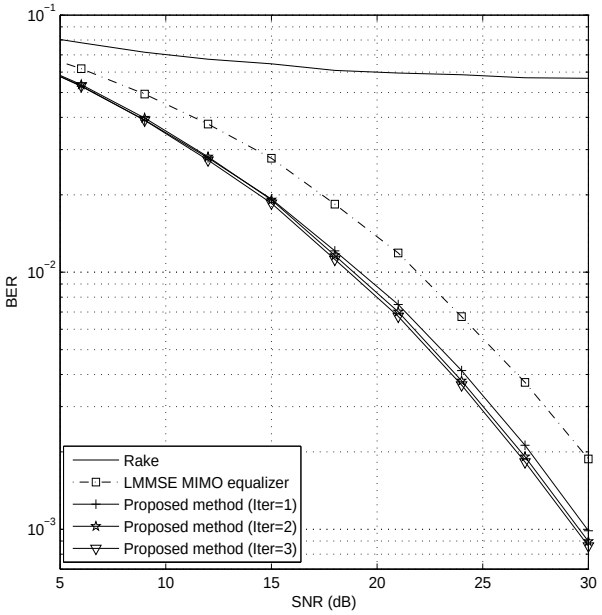

Fig. 4. BER performance for SNR variation.

Fig. 4 shows the BER performance of conventional methods [17] including the Rake and LMMSE MIMO equalizer as well as the proposed method. Due to the existence of strong interstream interference, we expect that the proposed approach outperforms the conventional MIMO equalizer. Also, as mentioned in Section III.A, we expect that the gain obtained per iteration diminishes so that most of gain is achieved at the first and second iterations. For example, at 0.5% BER, the proposed method achieves about 2.5 dB (after first iteration) and 3 dB (after second iteration) gain when compared with the LMMSE equalizer, while the gain after the third iteration is almost same as that of the second iteration.

In Fig. 5, we check the performance of the LMMSE equalizer and the proposed method for various slicing options.

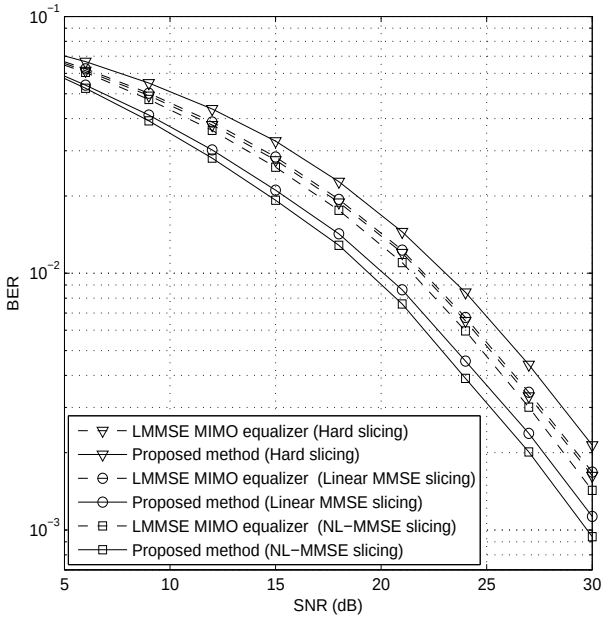

Fig. 5. BER performance of proposed method for various slicing options (Iter=1).

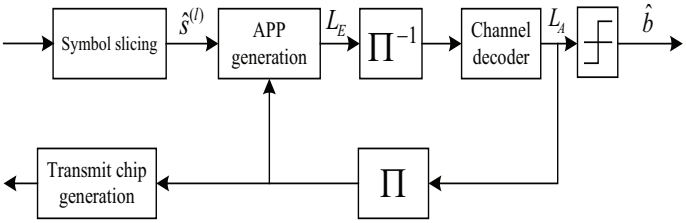

Fig. 6. The structure of proposed method employing channel decoder. L_E, and L_A are a priori information and extrinsic information of the decoder, respectively, and $\hat{b}$ is the decoded binary bit.

In our experiment, we test the soft slicing (nonlinear MMSE slicing), linear MMSE slicing, and hard slicing. These results clearly demonstrate that the performance of the proposed approach depends strongly on the symbol estimation quality. Specifically, when the hard slicing is employed, the proposed approach suffers almost 1 dB loss over the conventional MIMO equalizer because the accumulation of the estimation error induces error propagation. In contrast, as the NL-MMSE slicing moderates the effect of error propagation by suppressing unreliable symbols, the proposed scheme with the NL-MMSE slicing outperforms that with the linear MMSE slicing and hard slicing as well as the conventional MIMO equalizer.

Finally, we check the performance of the proposed scheme when a channel decoder is employed. In this case, as shown in Fig. 6, the APP generation, interleaver (deinterleaver), and the channel decoder are additionally required between the soft symbol slicer and transmit chip generator. As a channel decoder, standard 3GPP half rate ($r = 1/2$) Turbo code with $g_0(D) = 1 + D^2 + D^3$ and $g_1(D) = 1 + D + D^3$ is employed [1] and the iteration number of the Turbo decoder is set to 8. Fig. 7 shows the BER performance of the proposed

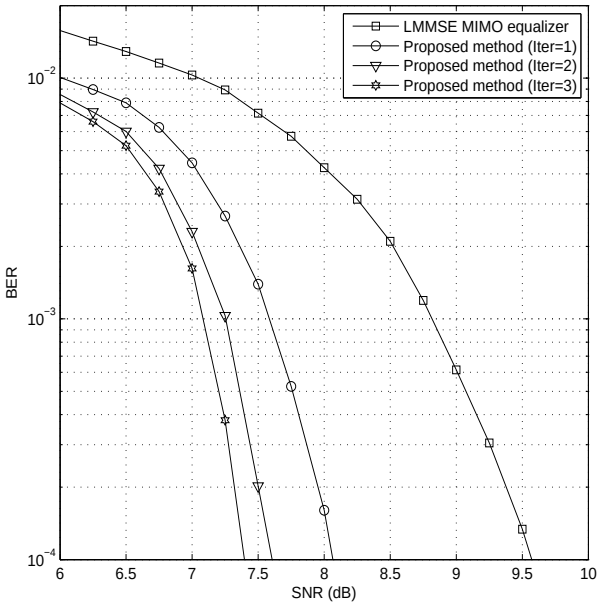

Fig. 7. BER performance of the proposed method with channel decoding.

method employing channel decoding. Since the scheme with the channel decoder generates symbols with improved error performance, re-generated interstream interferences becomes more accurate, and hence the effective channel gets closer to the SIMO channel. Indeed, as shown in Fig. 7, the proposed method brings significantly better algorithmic gain as well as the diversity gain than the scheme without decoder. For example, at 0.01% BER, the gain of the proposed method over the conventional MIMO equalization is 1.5 dB after the first iteration, and that increases to 2 and 2.3 dB after the second and third iterations, respectively.

V. Conclusion

The main purpose of this work is to provide an interstream interference cancellation strategy for CDMA system with frequency selective MIMO channels. Motivated by the fact that the SIMO equalizer is more robust to ill-behavior of channel than MIMO equalizer, we employed the iterative interstream interference cancellation and SIMO equalization for improving the performance of MIMO-CDMA systems. From the simulation on downlink of HSPA+ system, we observed that the proposed method achieves substantial gain over the conventional LMMSE MIMO equalization. Other than the HSPA+ applications primarily considered in this paper, the proposed method can be applied to any system under frequency selective MIMO channels (e.g., single-carrier frequency domain equalization [10] in LTE-uplink)

References

[1] 3rd Generation Partnership Project; Technical Specification Group Radio Access Network; Physical layer (Rel. 9) Tech. Spec. 25.201.V9.0.0, 2009. (http://www.3gpp.org/ftp/Specs/archive/25_series/25.201/25201-900.zip)

[2] G. J. Foschini, "Layered space time architecture for wireless communication in a fading environment when using multi-element antennas," *Bell labs Tech. J.*, vol. 1, pp. 41-59, 1996.

[3] N. Boubaker, K. B. Letaief, and R. D. Murch, "Performance of BLAST over frequency-selective wireless communication channels," *IEEE Trans. Commun.*, vol. 50, pp. 196-199, Feb. 2002.

[4] T. Abe, and T. Matsumoto, "Space-time turbo equalization in frequency-selective MIMO channels," *IEEE Trans. Veh. Technol.*, vol. 52, pp. 469-492, May 2003.

[5] S. Bäro, J. Hagenauer, and M. Witzke, "Iterative detection of MIMO transmission using a list sequential (LISS) detector," *IEEE International Conference on Commun. (ICC)*, vol. 4, pp. 2653-2657, May 2003.

[6] S. M. Sadough, M. A. Khalighi, and P. Duhamel, "Improved Iterative MIMO Signal Detection Accounting for Channel-Estimation Errors," *IEEE Trans. Veh. Technol.*, vol. 58, pp. 3154-3167, Sep. 2009.

[7] J. Ylioinas, and M. Juntti, "Iterative joint detection, decoding, and channel estimation in turbo coded MIMO-OFDM," *IEEE Trans. Veh. Technol.*, vol. 58, pp. 1784-1796, May 2009.

[8] B. Hochwald and S. ten Brink, "Achieving near-capacity on a multiplean-tenna channel," *IEEE Trans. Commun.*, vol. 51, no. 3, pp. 389-399, Mar. 2003.

[9] Z. Guo and P. Nilsson, "Algorithm and implementation of the K-best sphere decoding for MIMO detection," *IEEE J. Sel. Areas Commun.*, vol. 24, pp. 491-503, Mar. 2006.

[10] D. Falconer, S. L. Ariyavisitakul, A. Benyamin-Seeyar, and B. Eidson, "Frequency Domain Equalization for Single-Carrier Broadband Wireless Systems," *IEEE Commun. Magazine*, vol. 40, pp. 58-66, Apr. 2002.

[11] A. V. Oppenheim, *Discrete-time signal processing*, Prentice Hall, Inc. 1999.

[12] S. M. Kay, *Fundamentals of statistical signal processing: estimation theory*, Prentice Hall, Inc. 1993.

[13] R. D. Yates and D. J. Goodman, *Probability and stochastic processes*, Johns Wiley and Sons, Inc. 2005.

[14] G. H. Golub and C. F. V. Loan, *Matrix computations*, Johns Hopkins University Press, 1996.

[15] J. G. Proakis, *Digital Communications*, 3rd ed. McGraw-Hill, 1995.

[16] Guidelines for the evaluation of radio transmission technologies for IMT-2000, recommandation ITU-R M.1225, 1997.

[17] S. Haykin and M. Moher, *Moden wireless communications*, Prentice Hall, 2005.